CARBON letters

Note

Carbon Letters Vol. 16, No. 4, 281-285 (2015)

Effect of nickel on hydrogen storage behaviors of carbon aerogel hybrid

Ye-Ji Han and Soo-Jin Park*

Department of Chemistry, Inha University, Incheon 22212, Korea

Key words: carbon aerogels, nickel deposition, hydrogen storage

Article Info

Received 14 March 2015
Accepted 20 June 2015

***Corresponding Author**
E-mail: sjpark@inha.ac.kr
Tel: +82-32-876-7234

Open Access

DOI: http://dx.doi.org/10.5714/CL.2015.16.4.281

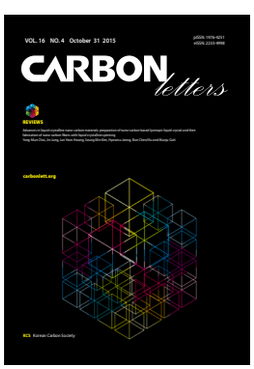

http://carbonlett.org

pISSN: 1976-4251
eISSN: 2233-4998

Limited conventional energy resources and serious environmental calamities have motivated researchers to find new and efficient sources of energy. The considerable efforts devoted to this end include the development of bio-diesel, solar cells, coal liquefaction/gasification technologies, and fuel cells. Hydrogen is considered by many an ideal energy source owing to its renewable and clean energy characteristics. In addition, it mostly produces water, which is eco-friendly compared to the byproducts of many other energy sources [1-6]. To use hydrogen as an energy source, various hydrogen storage methods such as the use of metal hydrides, liquefied hydrogen, and adsorption of hydrogen in porous materials have been studied [7-14]. The adsorption of hydrogen in porous materials is particularly suitable for hydrogen storage, which is critical for suitably utilizing hydrogen energy, owing to the reversibility and stability of this method. To date, the wide ranging attempts to develop hydrogen storage mechanisms include studies on carbon materials [15-17], metal-organic frameworks, and zeolites [18-21]. Carbon materials offer many advantages for hydrogen storage, such as easy preparation, suitable surface functional groups, low mass density, thermal stability, and hydrophobicity [22-24]. Carbon aerogels (CAs) in particular have been recognized as potential hydrogen storage materials because of their suitable structural properties, controllable mass densities, high specific surface areas, and mesopore volumes. However, it is necessary to modify the surfaces of carbon materials in order to reach the hydrogen storage capacities determined by the US Department of Energy (DOE).

Carbon materials containing transition metals such as platinum, copper, vanadium, and nickel exhibit attractive hydrogen storage properties [10,22,25]. Nickel is particularly promising since it is easily obtained on Earth, and it is inexpensive compared to other metals and enhances hydrogen storage properties. Improved hydrogen storage capacities have been obtained with nickel-plated porous carbon nanofibers owing to the spillover of hydrogen molecules onto the metal-carbon interfaces. In general, the presence of nickel particles on carbon materials has been shown to enhance the hydrogen storage capacity [3,9,19].

In this work, CAs were chemically activated by KOH to produce well-developed pore structures and ultimately increase the hydrogen storage capacities. Nickel-loaded activated carbon aerogels (ACAs/Ni hybrid materials) with various nickel content were prepared. Ni particles were loaded onto ACAs to introduce hydrogen-favorable active sites onto the ACA surfaces and improve the hydrogen storage capacities.

The CAs were prepared using resorcinol as the carbon precursor and formaldehyde as the initiator. Resorcinol (7.5 g) was dissolved in a solution of distilled water (75 mL) and formaldehyde (25 g). Sodium carbonate was then added to this solution, and the mixture was stirred for 3 h in an open container and dried for 3 h at room temperature. Subsequently, the wet gel was dried at 80°C for 48 h and then immersed in an acetone solution for 24 h without stirring. The aerogels were obtained after drying at 80°C for 24 h. Prior to use, the aerogels were carbonized in a furnace with a heating rate of 2°C min^{-1} under a N_2 gas atmosphere. The CAs were treated with KOH solution at 60°C overnight, with a KOH/CA mass ratio of 2:1. The prepared KOH/CA mixtures were then heated to 900°C in a furnace under a N_2 gas flow (heating rate 2°C min^{-1}, flow rate 200 cm^3/min). The resulting products were then washed

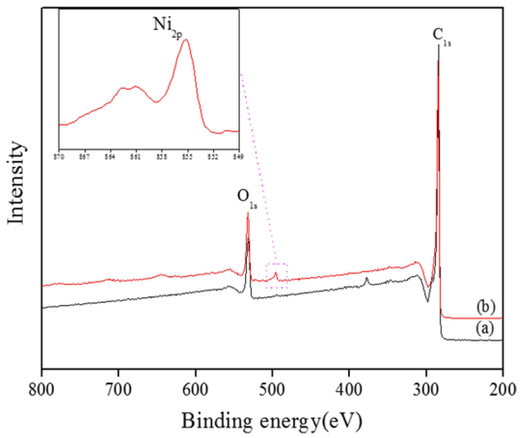

Fig. 1. X-ray photoelectron spectroscopy survey scan of (a) activated carbon aerogel (ACA) and (b) ACA/Ni hybrid materials.

Table 1. Textural properties of the prepared samples

Specimens	S_{BET} [a] (m^2/g)	V_{total} [b] (cm^3/g)	V_{meso} [c] (cm^3/g)	V_{micro} [d] (cm^3/g)	Ni content [e] (at%)
ACA	1364	1.130	0.569	0.561	-
ACA/Ni-0.2	1237	1.050	0.551	0.499	0.25
ACA/Ni-0.5	1216	1.055	0.561	0.494	0.75
ACA/Ni-1	1205	1.032	0.547	0.485	1.25
ACA/Ni-2	1182	0.991	0.514	0.477	1.60

ACA: activated carbon aerogel.
[a] S_{BET}: Specific surface area computed using Brunauer-Emmett-Teller equation at a relative pressure range of 0.0002-0.1. [b] V_{Total}: total pore volume is estimated at a relative pressure $P/P_0 = 0.99$. [c] V_{Meso}: mesopore volume determined from the Barrett-Joyner-Halenda equation. [d] V_{Micro}: micropore volume determined by subtracting the mesopore volume from the total pore volume. [e] Ni content: Ni content is characterized by X-ray photoelectron spectroscopy.

with distilled water until a neutral pH was attained. The samples were dried in an oven at 80°C for 24 h to obtain the ACAs.

To synthesize the ACA/Ni hybrid materials, the ACA was added to 100 mL of ethylene glycol and ultrasonicated for 1 h. Nickel sulfate hexahydrate (0.2, 0.5, 1, and 2 wt% of $NiSO_4 \cdot 6H_2O$ per 1 g of ACA) was dissolved in ethylene glycol and the solution was mechanically stirred for 4 h. NaOH was added to adjust the pH of the solution to neutral values. To remove oxygen and the organic byproducts, formaldehyde was added and stirred at 90°C for 2 h under an Ar atmosphere. Finally, the ACA/Ni hybrid materials were washed with de-ionized water and dried in a vacuum oven for 24 h [3].

X-ray photoelectron spectroscopy (XPS) measurements were conducted with a monochromated Al Kα X-ray source. Survey scans for Ni_{2p} were shown in the 854-859 eV binding energy range, with a pass energy of 0.1 eV. A non-linear least squares curve-fitting program (Peak-Fit version 4) with a Gaussian-Lorentzian mix function and Shirley background subtraction was employed to interpret the XPS peaks. To examine the porous textural characteristics of the samples, N_2/77 K adsorption-desorption isotherms were obtained using a Belsorp Max instrument (BEL Japan, Inc., Toyonaka, Japan). The samples were degassed at 473 K for 6 h to reduce the residual pressure below 10^{-6} mmHg. The specific surface areas were calculated using the Brunauer-Emmett-Teller (BET) equation. The micropore size distributions were obtained by applying the Horvath-Kawazoe (H-K) method.

The hydrogen storage measurements were conducted at 298 K/100 bar, conditions that are compatible with future electric-vehicle applications. Prior to the measurements, the samples in the chamber were degassed at 473 K for 12 h. After the chamber was cooled to room temperature, the samples were purged with flowing He and stored under a He atmosphere before further measurements. Hydrogen was supplied to the chamber until a pressure of 100 bar was achieved. Ultra-high-purity hydrogen gas (99.9999%) was used to exclude the influences of moisture and other impurities. Finally, the hydrogen storage capacity was determined by a volumetric measurement method.

An XPS analysis was carried out to obtain chemical species information of the ACA/Ni hybrid material. As shown in Fig. 1, the spectra of the ACA showed C_{1s} and O_{1s} peaks, but no Ni_{2p} peaks, whereas the spectra of the ACA/Ni hybrid materials exhibited C_{1s}, O_{1s}, and Ni_{2p} peaks. The presence of oxygen in the spectra is attributed to natural auto-oxidation. As shown in Table 1, the amount of surface Ni atoms gradually increased as the ACA/Ni ratio increased from 0.2 to 2.0. The intensities of the Ni_{2p} peaks in the survey spectra of the ACA/Ni hybrid materials were clearly higher than that of ACA, thus demonstrating that the ACA and nickel particles are hybridized.

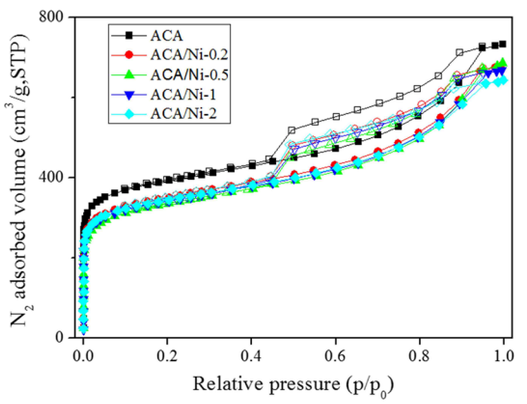

Fig. 2. N_2/77 K adsorption-desorption isotherms of the prepared samples. ACA: activated carbon aerogel, STP: standard temperature and pressure.

The N_2/77 K adsorption-desorption isotherms of the prepared samples with various nickel content are shown in Fig. 2. A typical type-IV isotherm with a hysteresis loop at relative pressure above 0.4 is observed, reflecting the influence of capillary condensation and the inter-tubular structure of the prepared samples [26,27]. While this type of isotherm indicates mesoporous materials, isotherms at a relative pressure below 0.1 are attributed to micropores, suggesting that the prepared samples are both mi-

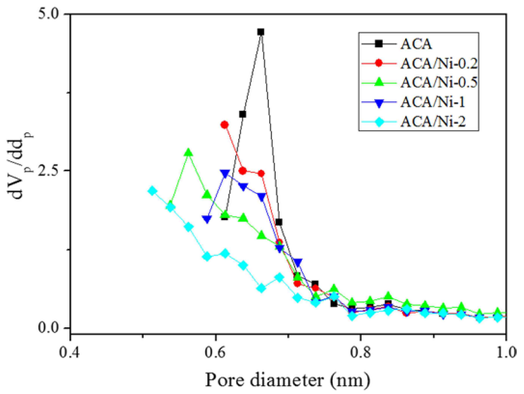

Fig. 3. Micropore size distributions of the prepared samples. ACA: activated carbon aerogel.

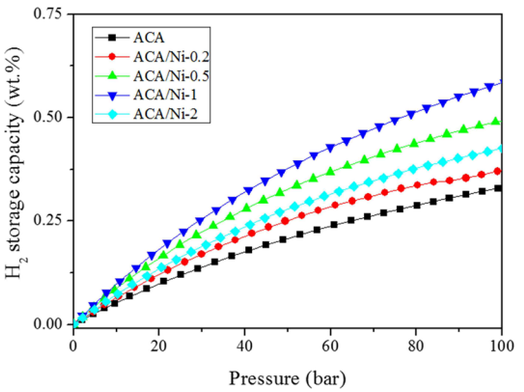

Fig. 4. Hydrogen storage capacities of the prepared samples. ACA: activated carbon aerogel.

croporous and mesoporous. The shapes of the isotherms of the ACA/Ni hybrid materials were consistent with the isotherm of the ACA. However, slight decreases in the specific area and total pore volume were observed owing to the blocking and filling of micropores and mesopores with nickel particles. The textural properties of the samples are shown in Table 1 to shed light on the pore structure. From these results, the adsorption volume, which depends on the specific surface area and total pore volume of the samples, gradually decreases as the nickel content increases, and this is ascribed to the nickel particles blocking the pores on the ACA surface.

Fig. 3 shows the micropore size distributions of the prepared samples with various amounts of nickel, determined using the H-K method. The micropore sizes ranged from 0.4 to 1.0 nm; this range also contains the optimal pore size range (0.6-0.7 nm) for hydrogen adsorption [28-30]. The micropore size distributions of the ACA were uniform, in contrast with those of the ACA/Ni hybrid materials. The results also showed that the the highest volume peaks of the prepared samples decreased in height as the nickel content increased.

The hydrogen storage capacities of ACA and ACA/Ni hybrid materials containing various amounts of nickel measured at 298 K/100 bar are shown in Fig. 4. The results show that the hydrogen storage capacities of the ACA/Ni hybrid materials are higher than that of the untreated ACA. Furthermore, the highest hydrogen storage capacity of the ACA/Ni hybrid materials (1 wt% of nickel per 1 g of ACA, ACA/Ni-1) is almost two times that of the untreated ACA. Normally, the hydrogen storage capacities of carbon materials depend strongly on the pore volume, specific surface area, and the accessible micropores where hydrogen adsorption mainly occurs. However, the results indicated that the hydrogen storage capacities of the ACA/Ni hybrid materials increased, despite that the micropore volume and specific surface area decreased because of the Ni particles on ACA. The above results clearly show that Ni particles are hydrogen-favorable sites by a spillover effect and enhance the hydrogen storage capacities of the ACA/Ni hybrid materials. In addition, in the case of metal-deposited adsorbents, charge transfer occurs between the metal and the adsorbent. The positively charged metal atoms polarize the hydrogen molecules, and the hydrogen molecules bond with the metal atoms. It is critical that hydrogen is adsorbed on the mesopores as well as the micropores. Both factors play an important role in determining the hydrogen storage capacity in the presence of Ni particles. Even though the pore volume and specific surface area decreased as a result of the blocking or filling of micropores, the adsorption of hydrogen atoms by the spillover effect is not affected by any blocking effect, as revealed by the improved hydrogen storage capacities [31-33]. These results show that the hydrogen storage capacities of ACA/Ni hybrid materials deposited with Ni (0.2, 0.5, and 1 wt% per 1 g of activated carbon aerogel) gradually increase as the Ni content steadily rise owing to adsorption in the presence of Ni. Thus, ACA/Ni-0.2 and 0.5 with low Ni content showed lower adsorptions than ACA/Ni-1. It was shown that the hydrogen storage capacity of ACA/Ni-2 decreased because of filling and blocking by the large amount of Ni particles. In conclusion, ACA/Ni-1 has optimum Ni content on the ACA surface and the nickel was well dispersed. Furthermore, ACA/Ni-1 has optimum pore size for hydrogen storage (as previously mentioned in Fig. 3).

Consequently, the highest hydrogen storage capacity of the ACA/Ni hybrid materials was 0.6 wt%, which was two times higher than that of untreated ACA. Although this is still lower than the goal established by the DOE, it nevertheless suggests the potential of carbon materials for hydrogen storage and an important relationship between the carbon material structure and suitable metals.

In this work, ACA/Ni hybrid materials were prepared by KOH activation of CAs and nickel nanoparticle deposition on ACAs in order to increase their hydrogen storage capacity. The specific surface area and micropore volume of the ACA decreased with the introduction of nickel owing to the pore blocking and filling effect of the Ni particles on the ACA surface. The hydrogen storage capacity of the untreated ACA sample was approximately 0.3 wt%, whereas that of the ACA/Ni-1 hybrid sample was 0.6 wt%. The presence of Ni particles introduced hydrogen-favorable sites, which can lead to an improved hydrogen storage capacity due to the catalytic characteristics of nickel. Based on these results, we suggest that ACA/Ni hybrid materials can potentially be used as hydrogen storage adsorbents given that the raw materials are easily obtainable and inexpensive.

Acknowledgments

This work was supported by the Industrial Strategic Technology Development Program (10050953) funded by the Ministry of Trade, Industry & Energy (MI, Korea).

References

[1] Schlapbach L, Züttel A. Hydrogen-storage materials for mobile applications. Nature, **414**, 353 (2001). http://dx.doi.org/10.1038/35104634.

[2] Liu C, Fan YY, Liu M, Cong HT, Cheng HM, Dresselhaus MS. Hydrogen storage in single-walled carbon nanotubes at room temperature. Science, **286**, 1127 (1999). http://dx.doi.org/10.1126/science.286.5442.1127.

[3] Kim BJ, Park SJ. Optimization of the pore structure of nickel/graphite hybrid materials for hydrogen storage. Int J Hydrogen Energy, **36**, 648 (2011). http://dx.doi.org/10.1016/j.ijhydene.2010.09.097.

[4] Wang J, Senkovska I, Kaskel S, Liu Q. Chemically activated fungi-based porous carbons for hydrogen storage. Carbon, **75**, 372 (2014). http://dx.doi.org/10.1016/j.carbon.2014.04.016.

[5] Im JS, Park SJ, Kim TJ, Kim YH, Lee YS. The study of controlling pore size on electrospun carbon nanofibers for hydrogen adsorption. J Colloid Interface Sci, **318**, 42 (2008). http://dx.doi.org/10.1016/j.jcis.2007.10.024.

[6] Zhu Y, Liu Z, Yang Y, Gu H, Li L, Cai M. Hydrogen storage properties of Mg-Ni-C system hydrogen storage materials prepared by hydriding combustion synthesis and mechanical milling. Int J Hydrogen Energy, **35**, 6350 (2010). http://dx.doi.org/10.1016/j.ijhydene.2010.03.094.

[7] Kim BJ, Lee YS, Park SJ. Novel porous carbons synthesized from polymeric precursors for hydrogen storage. Int J Hydrogen Energy, **33**, 2254 (2008). http://dx.doi.org/10.1016/j.ijhydene.2008.02.019.

[8] Silambarasan D, Surya VJ, Vasu V, Iyakutti K. Single walled carbon nanotube-metal oxide nanocomposites for reversible and reproducible storage of hydrogen. ACS Appl Mater Interfaces, **5**, 11419 (2013). http://dx.doi.org/10.1021/am403662t.

[9] Kim BJ, Lee YS, Park SJ. A study on the hydrogen storage capacity of Ni-plated porous carbon nanofibers. Int J Hydrogen Energy, **33**, 4112 (2008). http://dx.doi.org/10.1016/j.ijhydene.2008.05.077.

[10] Im JS, Kwon O, Kim YH, Park SJ, Lee YS. The effect of embedded vanadium catalyst on activated electrospun CFs for hydrogen storage. Microporous Mesoporous Mater, **115**, 514 (2008). http://dx.doi.org/10.1016/j.micromeso.2008.02.027.

[11] Brooks KP, Semelsberger TA, Simmons KL, van Hassel B. Slurry-based chemical hydrogen storage systems for automotive fuel cell applications. ACS Appl Mater Interfaces, **268**, 950 (2014). http://dx.doi.org/10.1016/j.jpowsour.2014.05.145.

[12] Jung MJ, Kim JW, Im JS, Park SJ, Lee YS. Nitrogen and hydrogen adsorption of activated carbon fibers modified by fluorination. J Ind Eng Chem, **15**, 410 (2009). http://dx.doi.org/10.1016/j.jiec.2008.11.001.

[13] Song MY, Kwak YJ, Lee SH, Park HR, Kim BG. Hydrogen-storage properties of MgH_2-10Ni-2$NaAlH_4$-2Ti prepared by reactive mechanical grinding. J Ind Eng Chem, **20**, 1591 (2014). http://dx.doi.org/10.1016/j.jiec.2013.07.052.

[14] Fukuzumi S, Suenobu T. Hydrogen storage and evolution catalysed by metal hydride complexes. Dalton Trans, **42**, 18 (2013). http://dx.doi.org/10.1039/C2DT31823G.

[15] Dhand V, Prasad JS, Rhee KY, Anjaneyulu Y. Fabrication of high pressure hydrogen adsorption/desorption unit: adsorption study on flame synthesized carbon nanofibers. J Ind Eng Chem, **19**, 944 (2013). http://dx.doi.org/10.1016/j.jiec.2012.11.013.

[16] Liu C, Chen Y, Wu CZ, Xu ST, Cheng HM. Hydrogen storage in carbon nanotubes revisited. Carbon, **48**, 452 (2010). http://dx.doi.org/10.1016/j.carbon.2009.09.060.

[17] Lee SY, Park SJ. Comprehensive review on synthesis and adsorption behaviors of graphene-based materials. Carbon Lett, **13**, 73 (2012). http://dx.doi.org/10.5714/CL.2012.13.2.073.

[18] Cai J, Li L, Lv X, Yang C, Zhao X. Large surface area ordered porous carbons via nanocasting zeolite 10X and high performance for hydrogen storage application. ACS Appl Mater Interfaces, **6**, 167 (2014). http://dx.doi.org/10.1021/am403810j.

[19] Park SJ, Lee SY. A study on hydrogen-storage behaviors of nickel-loaded mesoporous MCM-41. J Colloid Interface Sci, **346**, 194 (2010). http://dx.doi.org/10.1016/j.jcis.2010.02.047.

[20] Klyamkin SM, Chuvikov SV, Maletskaya NV, Kogan EV, Fedin VP, Kovalenko KA, Dybtsev DN. High-pressure hydrogen storage on modified MIL-101 metal-organic framework. Int J Energy Res, **38**, 1562 (2014). http://dx.doi.org/10.1002/er.3175.

[21] Sumida K, Stück D, Mino L, Chai JD, Bloch ED, Zavorotynska O, Murray LJ, Dincă M, Chavan S, Bordiga S, Head-Gordon M, Long JR. Impact of metal and anion substitutions on the hydrogen storage properties of M-BTT metal-organic frameworks. J Am Chem Soc, **135**, 1083 (2013). http://dx.doi.org/10.1021/ja310173e.

[22] Kim BJ, Lee YS, Park SJ. Preparation of platinum-decorated porous graphite nanofibers, and their hydrogen storage behaviors. J Colloid Interface Sci, **318**, 530 (2008). http://dx.doi.org/10.1016/j.jcis.2007.10.018.

[23] He L, Melnichenko YB, Gallego NC, Contescu CI, Guo J, Bahadur J. Investigation of morphology and hydrogen adsorption capacity of disordered carbons. Carbon, **80**, 82 (2014). http://dx.doi.org/10.1016/j.carbon.2014.08.041.

[24] Jasminská N, Brestovič T, Puškár M, Grega R, Rajzinger J, Korba J. Evaluation of hydrogen storage capacities on individual adsorbents. Measurement, **56**, 219 (2014). http://dx.doi.org/10.1016/j.measurement.2014.07.002.

[25] Park SJ, Kim BJ, Lee YS, Cho MJ. Influence of copper electroplating on high pressure hydrogen-storage behaviors of activated carbon fibers. Int J Hydrogen Energy, **33**, 1706 (2008). http://dx.doi.org/10.1016/j.ijhydene.2008.01.011.

[26] Roussel T, Pellenq RJM, Bienfait M, Vix-Guterl C, Gadiou R, Béguin F, Johnson M. Thermodynamic and neutron scattering study of hydrogen adsorption in two mesoporous ordered carbons. Langmuir, **22**, 4614 (2006). http://dx.doi.org/10.1021/la0527386.

[27] Xia K, Gao Q, Wu C, Song S, Ruan M. Activation, characterization and hydrogen storage properties of the mesoporous carbon CMK-3. Carbon, **45**, 1989 (2007). http://dx.doi.org/10.1016/j.carbon.2007.06.002.

[28] Vix-Guterl C, Frackowiak E, Jurewicz K, Friebe M, Parmentier J, Béguin F. Electrochemical energy storage in ordered porous carbon materials. Carbon, **43**, 1293 (2005). http://dx.doi.org/10.1016/j.carbon.2004.12.028.

[29] Xia K, Gao Q, Song S, Wu C, Jiang J, Hu J, Gao L. CO_2 activation of ordered porous carbon CMK-1 for hydrogen storage. Int J Hydrogen Energy, **33**, 116 (2008). http://dx.doi.org/10.1016/j.

ijhydene.2007.08.019.
[30] Kim BJ, Park SJ. Influence of surface treatments on micropore structure and hydrogen adsorption behavior of nanoporous carbons. J Colloid Interface Sci, **311**, 619 (2007). http://dx.doi.org/10.1016/j.jcis.2007.03.049.
[31] Froudakis GE. Hydrogen interaction with single-walled carbon nanotubes: a combined quantum-mechanics/molecular-mechanics study. Nano Lett, **1**, 179 (2001). http://dx.doi.org/10.1021/nl015504p.
[32] Park SJ, Lee SY. Hydrogen storage behaviors of platinum-supported multi-walled carbon nanotubes. Int J Hydrogen Energy, **35**, 13048 (2010). http://dx.doi.org/10.1016/j.ijhydene.2010.04.083.
[33] Wang L, Yang RT. New sorbents for hydrogen storage by hydrogen spillover: a review. Energy Environ Sci, **1**, 268 (2008). http://dx.doi.org/10.1039/B807957A.